EUROPEAN ORGANIZATION FOR NUCLEAR RESEARCH

CERN-EP/80-08
29 January 1980

STUDY OF MASSIVE ELECTRON PAIR PRODUCTION AT THE CERN INTERSECTING STORAGE RINGS

C. Kourkoumelis and L.K. Resvanis
University of Athens, Athens, Greece

T.A. Filippas and E. Fokitis
National Technical University, Athens, Greece

A.M. Cnops, J.H. Cobb[1], R. Hogue, S. Iwata[2], R.B. Palmer, D.C. Rahm, P. Rehak and I. Stumer
Brookhaven National Laboratory[3], Upton, NY, USA

C.W. Fabjan, T. Fields[4], D. Lissauer[5], I. Mannelli[6], P. Mouzourakis, K. Nakamura[7], A. Nappi[6], W. Struczinski[8] and W.J. Willis
CERN, Geneva, Switzerland

M. Goldberg, N. Horwitz and G.C. Moneti
Syracuse University[9], Syracuse, NY, USA

and

A.J. Lankford[10]
Yale University, New Haven, Conn., USA

(Submitted to Physics Letters)

---

1) Now at Lancaster University, England.
2) Permanent address: Nagoya University, Nagoya, Japan.
3) Research under the auspices of ERDA.
4) Permanent address: Argonne National Laboratory, Argonne, Ill., USA.
5) Permanent address: Tel-Aviv University, Israel.
6) On leave of absence from the University of Pisa and INFN, Sezione di Pisa, Italy.
7) Permanent address: University of Tokyo, Japan.
8) Now at the Physikalisches Institut, Technische Hochschule, Aachen, Germany.
9) Work supported by the US National Science Foundation.
10) Now at the University of California, Berkeley, Calif., USA.

ABSTRACT

Data from a study of electron pairs produced in pp collisions ($\sqrt{s}$ = 53 and 63 GeV) are used to extend measurements of the scaling function down to $m/\sqrt{s} \simeq 0.07$ ($4.5 < m < 19$ GeV). The dilepton continuum can be described by the scaling formula

$$m^3 \left.\frac{d^2\sigma}{dmdy}\right|_{y=0} = (2.60 \pm 0.13) \times 10^{-32} \exp\left[(-2.0 \pm 0.7)\frac{m}{\sqrt{s}}\right]\left(1 - \frac{m}{\sqrt{s}}\right)^{9.7 \pm 0.4} \text{ cm}^2 \text{ GeV}^2 .$$

The average transverse momentum of dielectrons was found to be 1.43 ± 0.07 GeV, independent of mass (in the range $4.5 < m < 8.7$ GeV) and rising with $\sqrt{s}$. The angular decay distribution of the pairs was measured in the s-channel helicity system and found to behave like $1 + \alpha \cos^2 \theta$, where $\alpha = 1.15 \pm 0.34$. The angular decay of Υ at the same energies was found to have $\alpha = 0.31 \pm 0.35$.

We have studied the inclusive production of electron pairs at the CERN Intersecting Storage Rings (ISR) as a function of centre-of-mass energies from $\sqrt{s} = 30$ to $\sqrt{s} = 63$ GeV. Previous results of this experiment have been published on electron pair production over a wide mass range [1-4] as well as on the production of χ states identified in their J/ψ plus γ decay [5]. More information on the production of electron pairs through J/ψ and T decay appear in the following Letter.

The electron pairs are detected using four modules, each consisting of proportional chambers, plastic scintillator hodoscopes, lithium foil transition radiators followed by xenon linear proportional chambers which provided electron-hadron discrimination, and a lead/liquid-argon electromagnetic shower detector segmented laterally and longitudinally to provide measurement of the electron energy, and to achieve further rejection of hadrons. Each module covers 50° to 130° in polar angle and 40° in azimuth. A detailed description of the apparatus can be found elsewhere [6].

Two triggers were used concurrently to select events of interest. Both triggers required a localized energy deposit above a given threshold in at least two calorimeters simultaneously with a proton-proton interaction. One trigger used an energy threshold of about 1.5 GeV, and no other conditions. This gave efficiencies which are easy to determine but did not accept the lower energy electrons that are essential for studying the lower masses and electron angular distributions. These were provided by the "correlation" trigger, which demanded that showers of 0.75 GeV or more be correlated with a charged track.

The four modules were run in two configurations. One, optimized for back-to-back electrons and hence high-mass pairs, was run for luminosities of 0.459 and 8.52×10^{37} cm^2 s^{-1} at $\sqrt{s} = 53$ and 63 GeV. The other favoured electron pairs with opening angles somewhat smaller than 180°, and was run for luminosities of 0.095, 0.757, and 0.228×10^{37} cm^2 s^{-1} at $\sqrt{s} = 30$, 53, and 63 GeV. The combined geometrical and trigger acceptance as a function of dielectron mass and transverse momentum is shown in Fig. 1.

Inefficiencies in electron measurement can arise from the triggers, shower reconstruction inefficiency, and track reconstruction inefficiency, including the electron selection by transition radiation. These effects, and particularly the sharp energy variation near trigger thresholds, were determined from test beam measurements with a complete module [6]. However, a very valuable control from the data is obtained from study of the J/ψ. This narrow resonance is sufficiently prominent for it to be observed in the sample where one electron is stringently selected, and the other is selected only on the basis of a shower reconstruction, whose efficiency is relatively well known. The background under the J/ψ in this sample is easily subtracted, and a comparison with the number of events, less

background, for a given set of selection criteria that are carefully chosen *not* to be energy dependent, gives the corresponding efficiency. The track reconstruction efficiency, with no electron identification requirements, was 87%. Asymmetric decays of the J/ψ are very sensitive to the trigger efficiency near threshold. As should be expected, the J/ψ decay angular distribution does not manifest high powers of the cosine of the decay angle in the region where the efficiency of the trigger is well known ($|\cos\theta| < 0.7$) [7]. We have taken advantage of this fact to fix the exact value of the trigger efficiency in the lowest energy bin. With this check we are confident that decay distributions of higher mass pairs will be correctly described.

The main sources of our background are external and internal photon conversions, showers simulated by hadrons interacting in the calorimeter, and hadron tracks overlapping with electromagnetic showers. These are eliminated mainly by the requirement of minimum ionization, transverse and longitudinal shower distributions, and transition radiation generation, respectively. The number of events in a given mass and transverse momentum bin as a function of a continuous "stringency" parametrization of these requirements, corrected for the corresponding efficiency determined by the procedure described above, would be a constant if there were no background. It was observed to contain also a decreasing component, with a constant plateau for sufficiently stringent requirements. This is already attained for loose stringency for the mass intervals of the J/ψ and T. For intermediate masses and large transverse momenta, tighter stringency is required in order to reach the plateau. For some regions, for example for masses in the interval 1.1-2 GeV and large p_T, no plateau is obtained and we cannot quote a cross-section. The background component has a dependence on the stringency of the requirements, which is similar for different mass regions, aiding the estimation of background in the accepted data samples.

For example, in the mass interval $5 < m_{ee} < 6$ GeV for an over-all efficiency of dielectron identification, $\varepsilon = 0.11$, the residual background was estimated to be 30%. At higher masses, $8 < m_{ee} < 10$ GeV, for the same ε the level of the background is only 6%.

The energy calibration was continuously monitored by the injection of a known charge on each detector element. The π^0 mass as determined by each module in each ISR run is monitored, and an over-all calibration is based on electrons from the J/ψ. The mass resolution agrees well with the test beam measurement of $\sigma(E)/E = 0.09\, E^{-\frac{1}{2}}$ (E in GeV [6]) and with the observed width of the J/ψ.

Figure 1 shows the dielectron cross-section as a function of mass for the combined data at $\sqrt{s}$ = 53 and 63 GeV. A 50% uncertainty on the subtraction of the background was included in the error.

We wish to use these data to investigate scaling in $\sqrt{\tau} = m/\sqrt{s}$. Our present statistics and understanding of the background allow us to extend the cross-section down to $m/\sqrt{s} = 0.07$, which is the relevant region for the production of intermediate vector bosons at the new colliding beam machines. Figure 2 shows that scaling is approximately successful in the range $\sqrt{s}$ = 28-63 GeV. We have included for comparison the data of Kaplan et al. [8] at $\sqrt{s}$ = 28 GeV, and the low-mass data $1.5 < m < 2.4$ at $\sqrt{s}$ = 53 and 63 GeV of Clark et al. [8]. Our data agree well with the form

$$m^3 \left.\frac{d^2\sigma}{dmdy}\right|_{y=0} = (2.32 \pm 0.12) \times 10^{-32} \exp\left[(-11.6 \pm 0.5)\frac{m}{\sqrt{s}}\right] \text{cm}^2\ \text{GeV}^2 ,$$

(a χ^2 of 25 for 30 degrees of freedom).

All the data in fig. 2 covering a larger range of τ-values can be represented by:

$$m^3 \left.\frac{d^2\sigma}{dmdy}\right|_{y=0} = (2.60 \pm 0.13) \times 10^{-32} \exp\left[(-2.0 \pm 0.7)\frac{m}{\sqrt{s}}\right] \left(1 - \frac{m}{\sqrt{s}}\right)^{9.7 \pm 0.4} \text{cm}^2\ \text{GeV}^2 ,$$

(a χ^2 of 72 for 57 degrees of freedom).

This function is superimposed on Fig. 1, and shows that our data are in good agreement with universal scaling.

Additional insight into the Drell-Yan process has been obtained by study of the decay angular distributions and total transverse momentum of the dielectron system. We have studied the angular distributions of the dielectrons in two mass intervals: for the continuum $4.5 < m_{ee} < 8.7$ GeV and for the T region $8.7 < m_{ee} < 10.3$ GeV. Figures 3c and 3d show the angular acceptance for the two mass regions for $\langle p_T \rangle$ = 1.4 and 1.8 GeV, respectively.

Figure 3a shows the angular distribution of the dielectron continuum. A fit to the form $d\sigma/d\cos\theta = (1 + \alpha \cos^2\theta)$ gives $\alpha = 1.15 \pm 0.34$. The T region (fig. 3b) is flatter, with $\alpha = 0.79 \pm 0.40$. If the continuum events are subtracted, with an estimated T/continuum ratio 2.0 ± 0.5, one obtains $\alpha = 0.31 \pm 0.35$ for the T.

The average transverse momentum of the dielectron as a function of mass is evaluated using the acceptance shown in fig. 4b. One difficulty of this measurement is the increase in the fraction of background with p_T, although the data are, of course, corrected appropriately. As a check, we have evaluated $\langle p_T \rangle$ with and without a requirement on low multiplicity in the modules containing the electrons. The background is considerably lower for the low multiplicity sample. Although the sample must be somewhat biased, the hadrons recoiling against the electron pair do not usually go into the same module as the electrons.

Figure 4 a shows the distribution as a function of p_T for different mass intervals for the restricted sample, where no other tracks or shower enter the same module with the electron. A comparison shows that the low multiplicity sample underestimates $\langle p_T \rangle$ by 6 ± 4%. The data in fig. 4a were not corrected for this effect. A fit was made to the form $d\sigma/dp_T^2 = A \exp(-bp_T)$. The resulting $\langle p_T \rangle$*) is given in fig. 5 for the data with $\sqrt{s}$ = 53 and 63 GeV combined, together with other experiments at lower energies [9]. It can be concluded that $\langle p_T \rangle$ seems independent of mass, but shows a substantial increase with $\sqrt{s}$. The T region has higher average p_T than the continuum [9]**), in agreement with the observation of Yoh et al. [9] at $\sqrt{s}$ = 27.4 GeV.

We have extended the scaling measurement down to $m/\sqrt{s} \simeq 0.07$. The decay angular distribution of the dielectron system was found to behave like $1 + \cos^2\theta$ in good agreement with the virtual photon production picture. The scaling and the angular distributions are consistent with a simple Drell-Yan mechanism for dilepton production [10].

However, a departure from the naïve Drell-Yan picture in support of QCD [11] corrections, is found for the average transverse momentum behaviour: it was measured to be independent of mass for fixed $\sqrt{s}$ and to rise with $\sqrt{s}$ for fixed τ.

---

*) The $\langle p_T \rangle = 2/b$ were also consistent with a straight weighted average on the p_T. We have measured
$\langle p_T \rangle = 1.42 \pm 0.20$ GeV for $4.0 < m < 4.5$ GeV;
$\langle p_T \rangle = 1.46 \pm 0.10$ GeV for $4.5 < m < 5.0$ GeV;
$\langle p_T \rangle = 1.42 \pm 0.09$ GeV for $5.0 < m < 6.0$ GeV;
$\langle p_T \rangle = 1.43 \pm 0.09$ GeV for $6.0 < m < 8.7$ GeV;
$\langle p_T \rangle = 1.78 \pm 0.13$ GeV for $8.7 < m < 10.3$ GeV.

**) See discussion in the subsequent paper.

REFERENCES

[1] J.H. Cobb et al., Phys. Lett. 68B (1977) 101.

[2] J.H. Cobb et al., Phys. Lett. 72B (1977) 273.

[3] C. Kourkoumelis et al., BNL 25075, contributed to the 19th Int. Conf. on High-Energy Physics, Tokyo, 1978.

[4] J.H. Cobb et al., Phys. Lett. 78B (1978) 519.

[5] J.H. Cobb et al., Phys. Lett. 72B (1978) 497.
C. Kourkoumelis et al., Phys. Lett. 81B (1979) 405.

[6] J.H. Cobb et al., Nucl. Instrum. Methods 140 (1977) 413; 159 (1979) 93.
C. Kourkoumelis, CERN 77-06 (1977).
A.J. Lankford, CERN EP Internal Report 78-03 (1978).

[7] K.J. Anderson et al., Phys. Rev. Lett. 42 (1979) 944 (the angular decay distribution of the J/ψ was observed to be flat in πp interactions).

[8] D.K. Kaplan et al., Phys. Rev. Lett. 40 (1978) 435.
A.J. Clark et al., Nucl. Phys. B142 (1978) 29.
The confirmation of resonances in the mass region 1.5 to 2.4 GeV may question the use of these data as continuum.

[9] J.G. Branson et al., Phys. Rev. Lett. 38 (1977) 1334.
J.K. Yoh et al., Phys. Rev. Lett. 41 (1978) 684.

[10] G. Altarelli, Proc. EPS Int. Conf. on High-Energy Physics, Geneva, 1979 (CERN, Geneva, 1980), p. 727.

[11] I. Hinchliffe and Ch. Llewellyn Smith, Phys. Lett. 66B (1977) 281.
A.V. Radyushkin, Phys. Lett. 69B (1977) 245.
G. Altarelli et al., Phys. Lett. 76B (1978) 351 and 356.

Figure captions

Fig. 1 : The cross-section $(d^2\sigma/dmdy)_{y=0}$ versus mass for the data at $\sqrt{s}$ = 53 and 63 GeV combined. The curve is a result of the fit to the continuum displayed in fig. 2.
The inset shows the mass acceptance for "1977" and "1978" triggers and geometrical configurations calculated for isotropic decay distributions and production uniform in rapidity with p_T dependence $d\sigma/dp_T^2 \sim \sim \exp(-bp_T)$, where $b = 1.4\ GeV^{-1}$.
The mass acceptance changes by ±15% when the helicity decay distribution follows $dN/d\cos\theta = 1 + \alpha\cos^2\theta$ when $\alpha = \pm 1$, where θ is measured in the s-channel helicity frame.

Fig. 2 : Plot of $m^3(d^2\sigma/dmdy)_{y=0}$ for the electron pair continuum.

Fig. 3 : a) The angular distribution of the dielectron system after acceptance correction for the continuum region.
b) Same as (a) for the T region.
c) Angular acceptance for the continuum region assuming flat rapidity and $d^2\sigma/dp_T^2 \sim \exp(-bp_T)$, where $b = 1.4\ GeV^{-1}$.
d) Same as (c) for the T region; $b = 1.7\ GeV^{-1}$.
The curves of figs. 3a and 3b are a result of the fits to $dN/d\cos\theta \sim \sim 1 + \alpha\cos^2\theta$.

Fig. 4 : a) Plot of the acceptance corrected $d^2\sigma/dp_T^2$ versus p_T for different dielectron mass intervals. The line represents the result of the fit $d^2\sigma/dp_T^2 \sim \exp(-bp_T)$. The data at $\sqrt{s}$ = 53 and 63 GeV were combined.
b) Plot of the p_T acceptance calculated using $dN/d\cos\theta = 1 + \cos^2\theta$ for the decay angle of the dielectron system for the two running configurations combined.

Fig. 5 : $\langle p_T \rangle$ versus m for different energies. The average p_T in the J/ψ and T regions was calculated using both resonances and continuum.

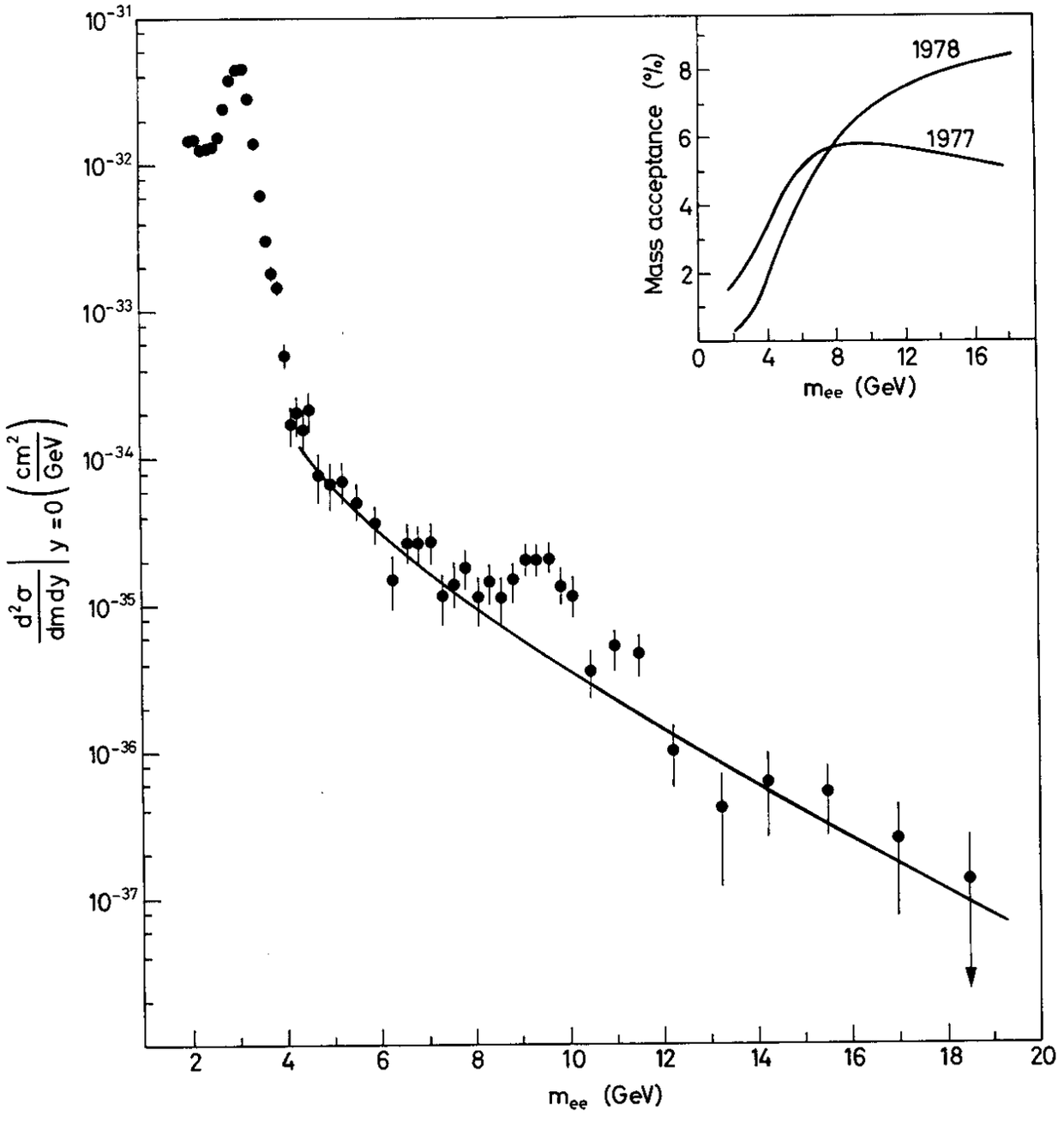
10^{-31}
10^{-32}
10^{-33}
10^{-34}
10^{-35}
10^{-36}
10^{-37}
$\frac{d^2\sigma}{dm\,dy}\Big|_{y=0}\left(\frac{cm^2}{GeV}\right)$
2
4
6
8
10
12
14
16
18
20
m_{ee} (GeV)
Mass acceptance (%)
1978
1977
0
4
8
12
16
m_{ee} (GeV)

Fig. 1

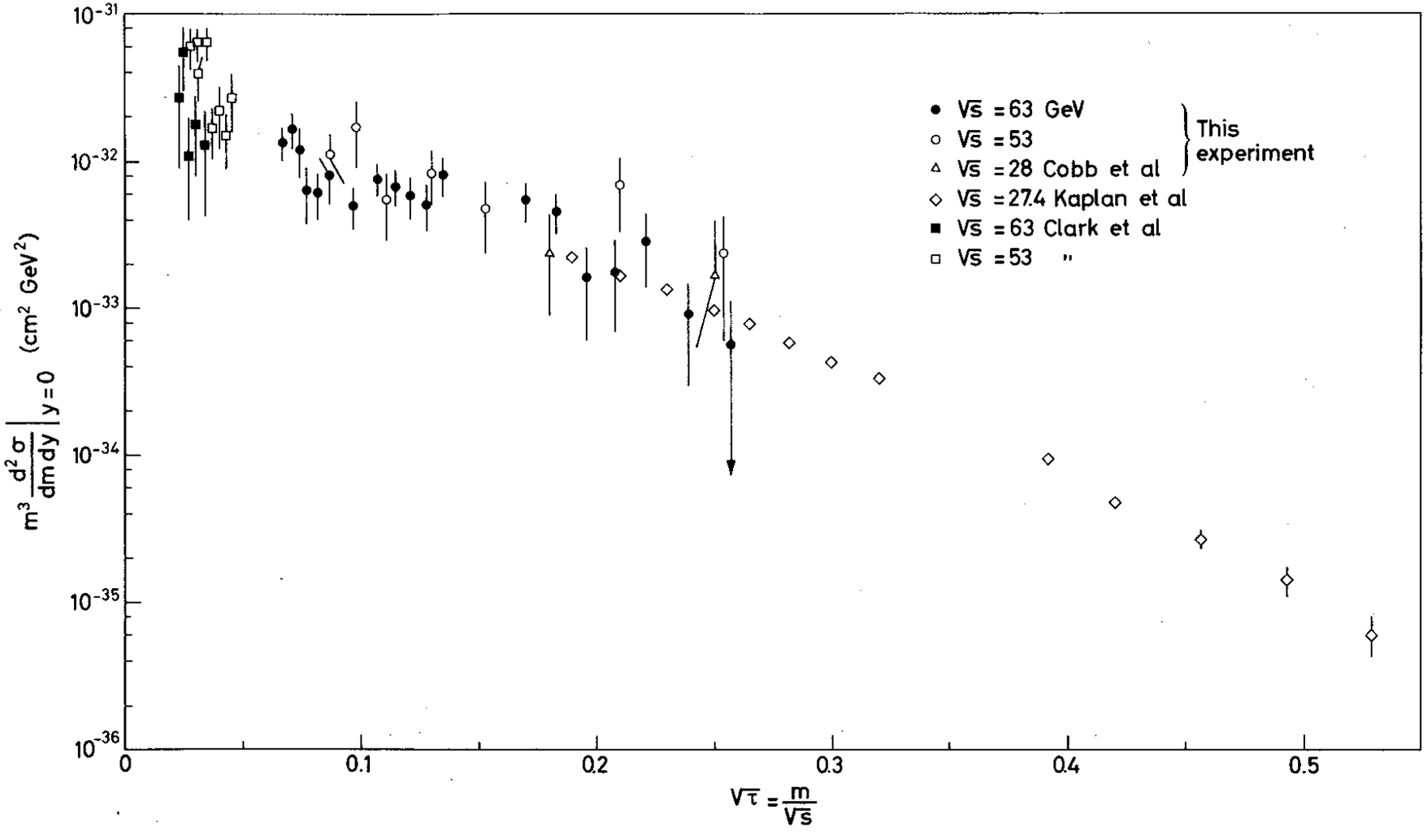
10^{-31}
10^{-32}
10^{-33}
10^{-34}
10^{-35}
10^{-36}
$m^3 \frac{d^2\sigma}{dm\,dy}\Big|_{y=0}$ (cm² GeV²)
0
0.1
0.2
0.3
0.4
0.5
$V\tau = \frac{m}{\sqrt{s}}$
● √s = 63 GeV
○ √s = 53
△ √s = 28 Cobb et al
◇ √s = 27.4 Kaplan et al
■ √s = 63 Clark et al
□ √s = 53 "
This experiment

Fig. 2

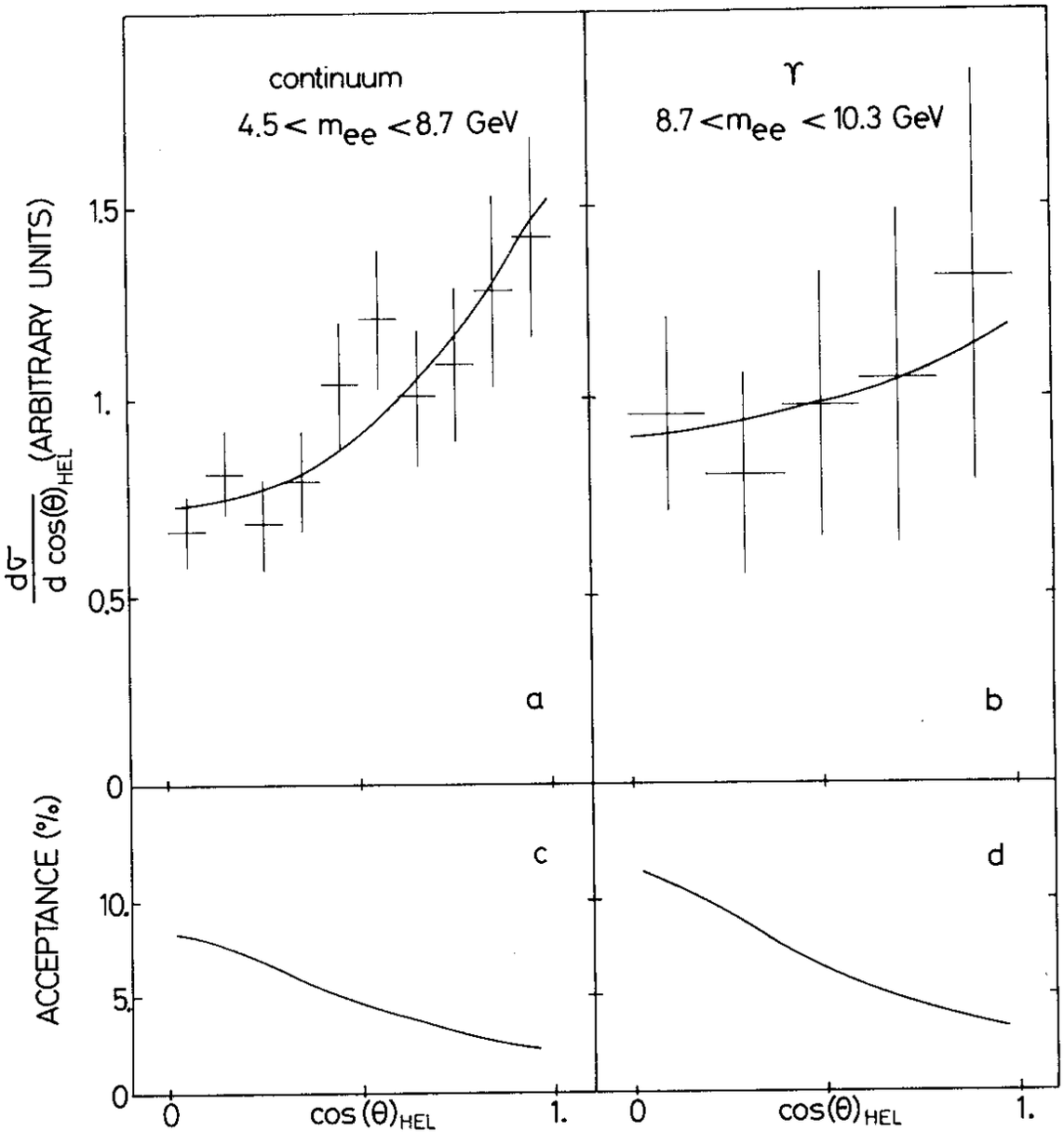
continuum
4.5 < m_ee < 8.7 GeV
Υ
8.7 < m_ee < 10.3 GeV
dσ/d cos(θ)_HEL (ARBITRARY UNITS)
1.5
1.
0.5
0
a
b
ACCEPTANCE (%)
10.
5.
0
c
d
0
cos(θ)_HEL
1.
0
cos(θ)_HEL
1.

Fig. 3

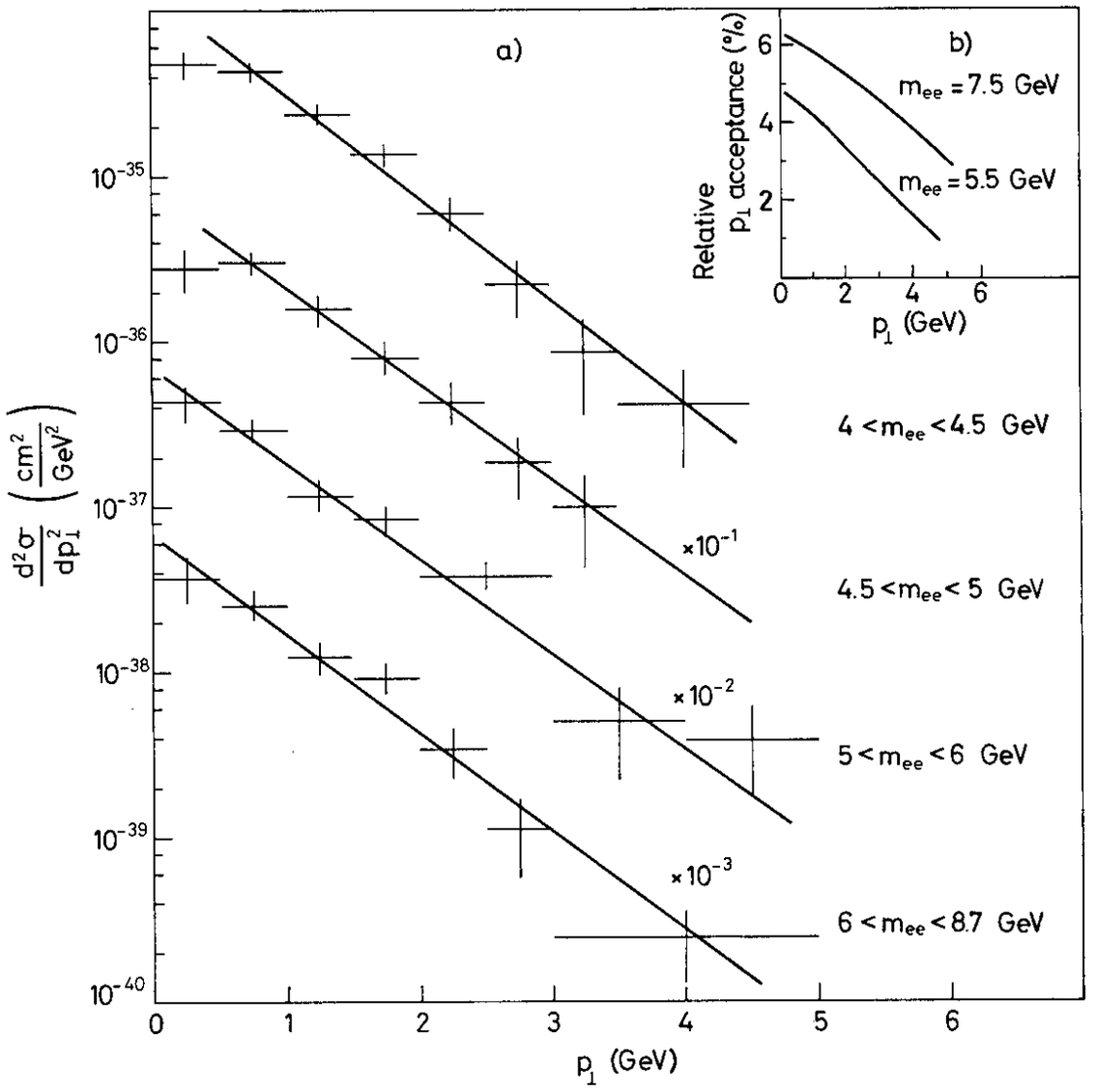
a)
b)
m_{ee} = 7.5 GeV
m_{ee} = 5.5 GeV
Relative $p_\perp$ acceptance (%)
$p_\perp$ (GeV)
$\frac{d^2\sigma}{dp_\perp^2}\left(\frac{cm^2}{GeV^2}\right)$
$4 < m_{ee} < 4.5$ GeV
$\times 10^{-1}$
$4.5 < m_{ee} < 5$ GeV
$\times 10^{-2}$
$5 < m_{ee} < 6$ GeV
$\times 10^{-3}$
$6 < m_{ee} < 8.7$ GeV
$p_\perp$ (GeV)

Fig. 4

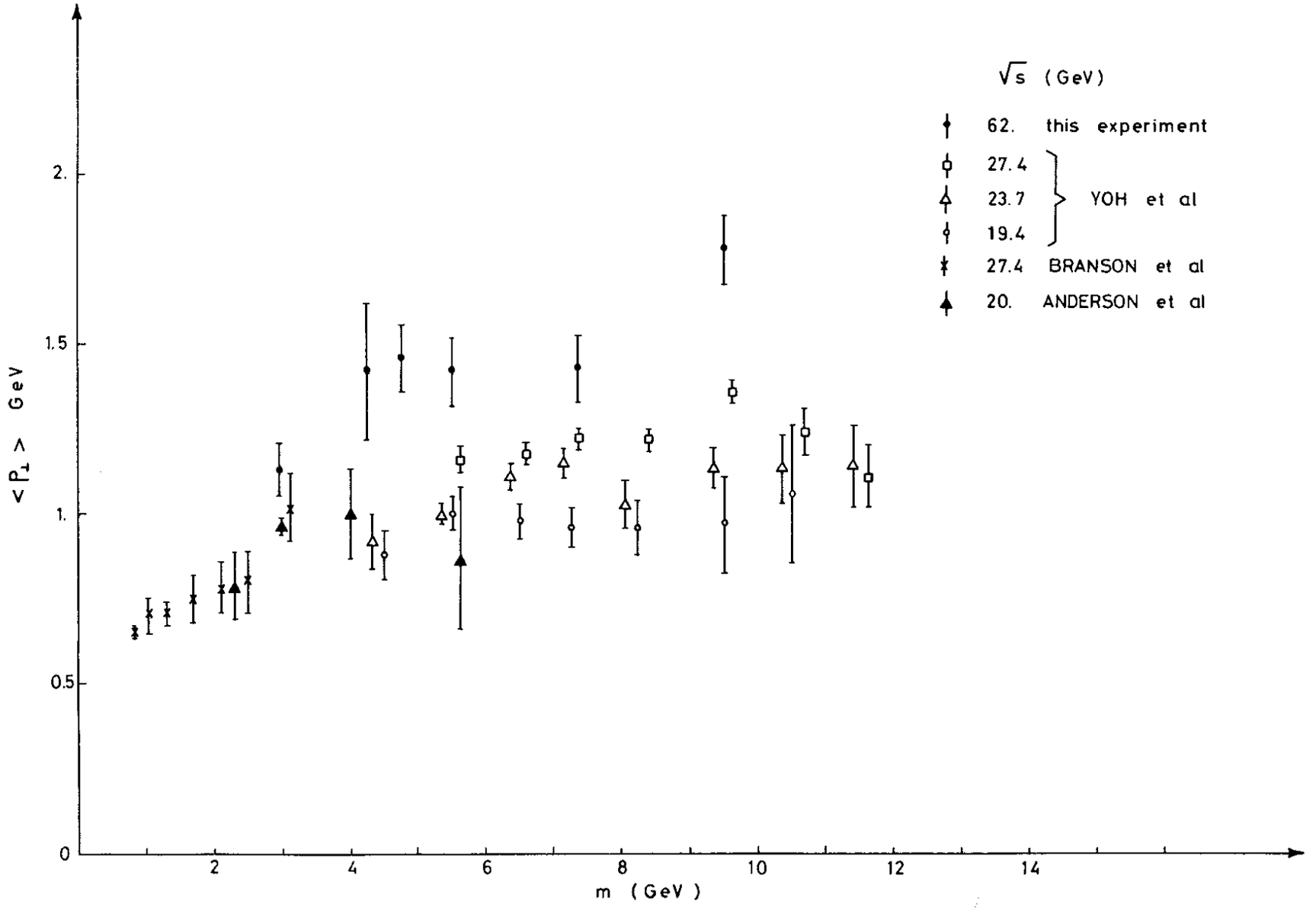
√s (GeV)
62. this experiment
27.4
23.7
19.4
YOH et al
27.4 BRANSON et al
20. ANDERSON et al
< P⊥ > GeV
0
0.5
1.
1.5
2.
2
4
6
8
10
12
14
m (GeV)

Fig. 5